

Mechanistic model for dispersion coefficients in bubble column

P.J. Skosana^a, D.S. van Vuuren^a, M.D. Heydenrych^b

^aMaterials Science and Manufacturing, CSIR, Pretoria

^bDepartment of Chemical Engineering, University of Pretoria, Pretoria

Keywords: Bubble column, model, circulation cell, dispersion coefficient

Abstract: A mechanistic model describing the mass and momentum exchange in bubble columns is proposed that is based on the observations that the gas distribution in a bubble column is not uniform across the column and that as a consequence large liquid recirculation cells are formed in such columns. The model provides insight into the mechanism of mass and momentum exchange in bubble columns and predicts turbulent viscosities in bubble columns that are similar to those reported in the literature. It also predicts axial and radial dispersion coefficients that are of the same order of magnitude as the reported data. Whereas the model is based on a description of the underlying physical phenomena, its validity and extrapolation is expected to be more reliable than that of empirical correlations.

INTRODUCTION

The Council for Scientific and Industrial Research (CSIR) is developing a novel continuous process to produce titanium metal powder. The technology initiated by the CSIR should benefit South Africa in achieving the long-term goal of establishing a competitive titanium (Ti) metal industry.

A bubble column reactor is one of the suitable reactor types that are being considered by the CSIR for the production of titanium. Depending on the application; bubble column reactors have several advantages over other multiphase reactors such as fluidised bed reactors, packed bed reactors, trickle bed reactors and continuous stirred tank reactors. These include, inter alia, the following (Joshi et al., 2002; Ruthiya, 2005; Tiefeng et al., 2007; Vinit, 2007; Singh & Majumder, 2010):

- Ease of construction since they contain only a cylindrical vessel, a gas distributor and a few internals
- Low maintenance costs due to the absence of moving parts
- Isothermal conditions
- High mass and heat transfer rates
- Online catalyst addition and removal
- Large liquid residence time which is suited to slow reactions
- Higher effective interfacial area and liquid mass transfer coefficients

Flow regimes encountered in bubble columns are classified as homogeneous and heterogeneous flow regimes (Shaikh & Al-Dahhan, 2005). In bubble columns operated in a heterogeneous flow regime, circulation cells are present which exchange momentum in a similar way to liquid eddies in the case of turbulent flow in a pipe. However, little work was done previously on the modelling of turbulent viscosities and dispersion coefficients caused by the momentum exchange of the circulation cells. In order to understand the fluid flow in bubble columns, a mechanistic model was developed and tested against results reported for the air–water system.

LITERATURE REVIEW

Models for dispersion coefficients

Ekambara & Joshi (1998) used the transient mass balance for a tracer in a two-dimensional axisymmetric cylindrical co-ordinate system. They assumed that the mixing process in a bubble column occurs due to transport at three levels, namely: molecular diffusion, eddy diffusion and bulk motion. Usually, the bulk motion is superimposed on either molecular or eddy diffusion or both and mixing can be characterized by the mean velocity components in the liquid phase. The dispersive transport can be characterized by eddy diffusivity in the liquid phase. In view of the controlling role of the convection and eddy diffusion, the solution of convection-diffusion equation for the liquid phase can give insight into the mechanism of axial mixing and hence a rational expression for the effective axial dispersion coefficient. Ekambara & Joshi (1998) developed a computational fluid dynamic (CFD) model for the prediction of flow patterns in terms of mean velocity and eddy diffusivity profiles. The validated CFD model was extended for the simulation of the macro-mixing process by incorporating the effects of both the bulk motion and the eddy diffusion. The model was further extended for the prediction of residence time distribution and hence the axial dispersion coefficient. The predicted values of axial dispersion coefficient were in good agreement with the experimental results from the literature.

Millies & Mewes (2005) explained that the main transport resistance for mixing of the liquid phase in a bubble column is located between different circulation cells where the liquid velocities are relatively small. They described each circulation cell as a stirred tank. They explained that liquid mixing mainly depends on the exchange rate of fluid elements between two consecutive circulation cells. This exchange rate was obtained as a result of the numerical calculation from the fluid dynamics. The liquid mixing was found to be proportional to the square root of the liquid circulation velocity. Millies & Mewes (2005) explained that a structured model and a one-dimensional dispersion model may be obtained by simplifying the transport equation of tracer for the case of high aspect ratios. Thus, the coefficient of the structured model and the axial dispersion coefficient were estimated numerically.

The estimated axial dispersion coefficients were an order of magnitude smaller than experimental values. Thus, describing each circulation cell as a stirred tank was not appropriate as a link between the fluid dynamics and liquid mixing.

Degaleesan & Dudukovic (1998) performed a Taylor-type analysis of the fundamental two-dimensional axisymmetric convection-diffusion equation for liquid mixing in bubble columns. An expression for the effective axial dispersion coefficient in terms of convective recirculation, and axial and radial eddy diffusion was then derived. The analysis is restricted to systems with low superficial liquid velocities, where the cross-sectional average liquid velocity relative to local liquid velocities was negligible. The governing equation for the liquid-confined tracer, in the presence of assumed angular symmetry, is a two-dimensional convection-diffusion equation. This equation is only applicable in the well-developed flow region in the column (middle portion of the recirculation cell) of columns with a large aspect ratio. The analysis showed that the main contributing factors to liquid back mixing in bubble columns are liquid recirculation and eddy diffusion. The axial dispersion coefficient was represented as a sum of two terms (one that has the form of Taylor diffusivity and encompasses the contributions of liquid recirculation velocity and radial eddy diffusivity taking into account the liquid holdup profile, and the cross-sectional mean axial eddy diffusivity).

Degaleesan et al. (1996) developed a Recirculation and Cross Flow with Dispersion (RCFD) model for liquid mixing in bubble columns. In this model, mixing of the liquid phase was considered to be primarily due to convective recirculation and turbulence caused by the rising gas bubbles. The RCFD model in an axisymmetric system was derived by dividing a bubble column axially into three sections, namely: a middle region and two end zones where the liquid turns around. For simplicity the end zones were assumed to be perfectly mixed. In the middle region liquid mixing was described by taking into account the recirculation of the liquid. This was done by dividing this region into two sections: one with liquid flowing up near the column centre (section 1) and another with liquid flowing down near the column wall (section 2). Turbulent axial mixing was accounted by an axial dispersion coefficient in each section, and radial mixing was incorporated into an exchange coefficient

between section 1 and 2. The input parameters of the model were obtained using non-invasive experimental techniques, such as Computer Automated Radioactive Particle Tracking (CARPT) and Computer assisted Tomography (CT) to measure the local liquid velocities and radial gas holdup. In addition, it was shown that model parameters can be related to the turbulent eddy diffusivity measurements obtained by CARPT. The RCFD model was shown to compare well with tracer data and to reflect a variety of experimental observations. The axial dispersion model also produced a good fit of tracer data, but resulted in a low value of the dispersion Peclet number, outside the range for which the axial dispersion model is normally recommended. In addition, axial dispersion model was incompatible with other experimental evidence.

Circulation patterns

Circulation cells occur in the heterogeneous flow regime. This is a high-interaction flow regime which is characterised by circulation cells and poly-dispersed bubbles. In this flow regime, gas holdup is non-uniformly distributed in the radial direction, as shown in Figure 1.

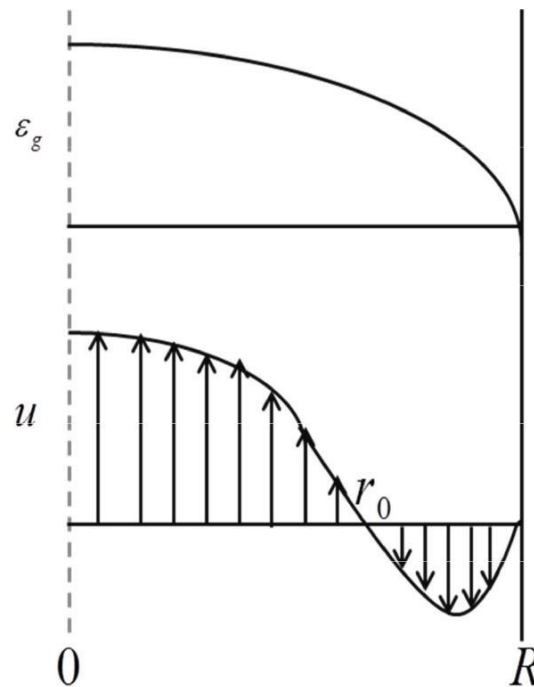


Figure 1: Schematic diagram of gas holdup and liquid velocity profile

The radial variation of gas holdup results in a variation of gravitational pressure in the radial direction, which increases from the column centre towards the column wall (Joshi et al., 2002). As a result, liquid circulation will develop because of gravitational pressure variations. In a circulation cell, the liquid flows in the upwards direction in the column centre and downwards near the column wall. The liquid flow is zero at r_0 before flowing down near the wall. r_0 is the radial position in the column where the liquid velocity is zero.

One of the causes of backmixing of the phases is liquid circulation. The rising bubbles in a bubble column carry the liquid in their wakes and in between them in the case of higher gas loading (Groen et al., 1996). The liquid carried by bubbles has to flow down and thus results in the liquid circulation. In the circulation loop of the reactor, the liquid rises through the centre and flows downwards near the column walls, as shown in Figure 2. Most of the gas bubbles rise up the column centre and leave the reactor at the top surface. However, smaller gas bubbles will circulate along with the liquid since they do not have enough buoyancy to disengage and leave the reactor (Gupta et al., 2001). The circulation mechanism is also facilitated by bubble–bubble interactions, bubble wakes and shear-induced turbulence. Phase circulation is considered to be the main course of backmixing.

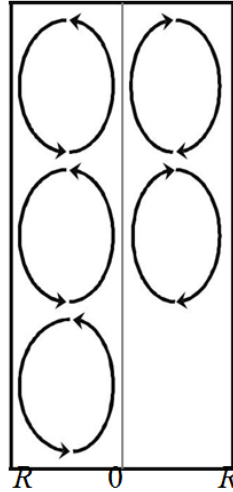


Figure 2: Liquid circulation patterns in bubble columns

MECHANISTIC MODEL DERIVATION

Liquid flow model

The mechanistic model is an extension of the approach proposed by Ueyama & Miyauchi (1979) who applied a force balance equation to develop a theoretical model for predicting the liquid velocity profile in a bubble column. Equation 1 is basically the sum of forces acting on liquid in a bubble column.

$$-\frac{1}{r} \frac{d}{dr} (r\tau) = \frac{dP}{dZ} + (1 - \varepsilon_G) \rho_L g \tag{1}$$

where r is a radial coordinate, τ is the shear stress, P is the pressure and Z is the axial coordinate.

The shear stress is given by:

$$\tau = -(\nu_M + \nu_t) \rho_L \left(\frac{du}{dr} \right) \tag{2}$$

where u is the interstitial liquid velocity, ρ_L is the liquid density, ν_M is the kinematic molecular viscosity and ν_t is the kinematic turbulent viscosity. Integrating Equation 1 between $r = 0$ and $r = R$ gives:

$$-\frac{dP}{dZ} = \left(\frac{2}{R} \right) \tau_w + (1 - \bar{\varepsilon}_G) \rho_L g \tag{3}$$

where $W \tau$ is the shear stress at the wall. Substituting Equations 3 and 2 into Equation 1 (neglecting ν_M in the turbulent core region of the bubble column), one obtains the modified basic equation for axial liquid flow in the turbulent core region:

$$-\frac{1}{r} \frac{d}{dr} \left(\nu_r \frac{du}{dr} \right) = \frac{2}{R \rho_L} \tau_w - (\bar{\varepsilon}_G - \varepsilon_G) g \tag{4}$$

Equation 4 can be solved by applying the following simplifying assumptions: (a) ν_t is constant throughout the turbulent core region, and (b) the profile of the gas holdup is approximated by Equation 5:

$$\frac{\varepsilon_G}{\bar{\varepsilon}_G} = \left[\frac{(n+2)}{n} \right] (1 - \phi^n) \tag{5}$$

The following boundary conditions apply for the turbulent core region:

$$\frac{du}{dr} = 0 \text{ at } r = 0$$

and

$$u = u_w \text{ at } r = R$$

The solution that satisfies the above boundary conditions is given by:

$$u + |u_w| = \frac{R^2}{\nu_t} \left[\left(\frac{\tau_w}{2R\rho_L} + \frac{\bar{\varepsilon}_G g}{2n} \right) (1 - \phi^2) - \frac{\bar{\varepsilon}_G g}{n(n+2)} (1 - \phi^{n+2}) \right] \tag{6}$$

If the gas holdup, the exponent in Equation 5 and the kinematic turbulent viscosity are known, there are still two unknowns in Equation 6, i.e. the shear stress at the wall and the liquid velocity of the turbulent core at the wall, that have to be determined before the liquid velocity profile can be calculated. The correlations to calculate the exponential factor, n , are not generally available. However, in the churn turbulent flow regime, the exponential levels off to a value of approximately 2 as the superficial gas velocity increases (Shaikh & Al-Dahhan, 2005).

To solve Equation 6 two additional requirements must be specified. The first is the liquid mass balance inside the column as given by:

$$\int_0^R \rho_L 2\pi r u (1 - \varepsilon_G) dr = 0 \tag{7}$$

Equation 7 implies that the net liquid mass flow rate is equal to zero for a bubble column operated in semi-batch mode.

In addition to this, Ueyama & Miyauchi (1979) used the universal velocity profile to model the laminar sub-layer at the wall, assuming that both the laminar sub-layer and the buffer layer consist of only liquid. The liquid velocity at surface of the sub-layer formed at the wall, $W u$, was thus predicted to be equal to:

$$u_w = 11.63 \sqrt{|\tau_w| / \rho_L} \text{ at } r = R$$

The algebraic solution to the system of equations is given in their paper.

Model for kinematic turbulent viscosity and dispersion coefficients

In this section, a mechanistic model for estimating the kinematic turbulent viscosity and dispersion coefficient is developed. A similar approach to that of Ueyama & Miyauchi (1979) was used in developing the model. The major difference is that, whereas Ueyama & Miyauchi (1979) determined the kinematic turbulent viscosities by fitting their liquid flow model to the reported data of liquid velocities, this work describes a way of estimating kinematic turbulent viscosity using a mechanistic model for the momentum exchange in bubble columns whereby the turbulent viscosity is product of

mass flux and the penetration depth. The turbulent viscosity is a function of the liquid flow patterns that cause momentum exchange between circulation cells. For ordinary molecular viscosity, the mechanism of momentum exchange is the random movement of molecules between different layers of flow which exchange momentum. In the case of turbulent flow on a larger scale, liquid eddies exchange momentum in a similar way to that of the molecules in viscous flow. In a bubble column, it is assumed that the circulation cells cause exchange of momentum.

Analogous to the kinetic gas theory for molecular viscosity or to the Prandtl mixing length theory for turbulent flow, the turbulent viscosity is defined as the product of the mass flux across the surface of a differential control volume and a penetration depth which is the distance that liquid in a circulation cell has to travel before it acquires the same momentum as that of the liquid in its new environment.

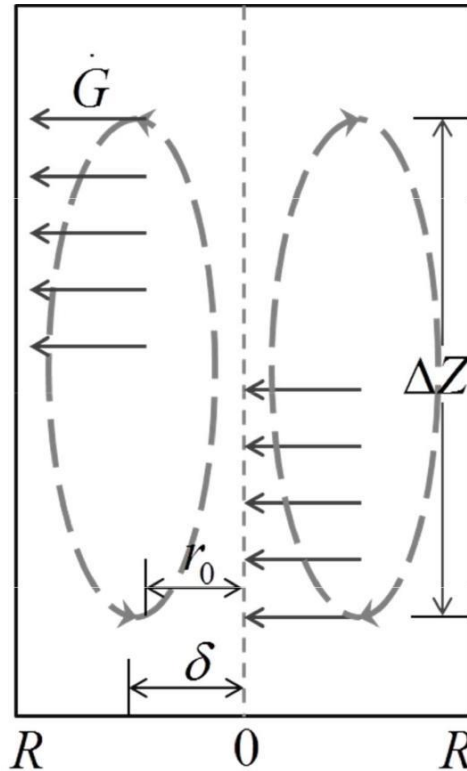


Figure 3: Schematic diagram depicting the momentum exchange between circulation cells

Figure 3 shows the mechanism of momentum exchange in bubble columns. In order to estimate the turbulent viscosity, the mass flux, G , across the curved surface where the liquid velocity is zero is used. The turbulent viscosity is the product of this mass flux and the distance that has to be travelled by a lump of fluid for it to change momentum, δ , as given by:

$$\mu_t = \delta G \tag{8}$$

The kinematic turbulent viscosity will therefore be estimated by:

$$\nu_t = \frac{\delta m_{upwards}}{2\pi r_0 \Delta Z \rho_L} \tag{9}$$

where upwards m is the liquid mass flowrate in the upward direction in the circulation cell, r_0 is the radius of the column in which the liquid velocity is zero and ΔZ is the height of the circulation cell. The cylindrical surface at r_0 is used to calculate G since the liquid flowing upwards with the flowrate upwards m has to cross

this curved surface area before flowing down. Joshi & Sharma (1979) used an energy balance technique to show that the energy of a recirculation cell is at a minimum when the height of the cell is equal to the diameter of the column. However, in this work, after comparing the model to data published in the literature when assuming that the exponential factor n equals 2, the height of the circulation cells was found to be approximately equal to 1.4 times the column diameter. The penetration depth is expected to be dependent on the column radius because the column wall confines the movement of the liquid and, therefore, the liquid is forced to change its momentum. The circulation cells are often symmetrical about the column centre; therefore, it was assumed that the penetration depth is approximately equal to half of the column radius. The upwards mass flow rate is calculated from:

$$m_{upwards} = \int_0^{r_0} 2\pi r \rho_L u (1 - \varepsilon_G) dr \tag{10}$$

Substituting $r_0 = R\phi_0$ and Equation 6 into Equation 10 and integrating gives:

$$m_{upwards} = -\pi R^2 \rho_L \phi_0^2 |u_w| + 2\pi R^2 \rho_L P \left(\frac{\phi_0^2}{2} - \frac{\phi_0^4}{4} \right) - 2\pi R^2 \rho_L N \left(\frac{\phi_0^2}{2} - \frac{\phi_0^{n+2}}{n+4} \right) + 2\pi R^2 \rho_L |u_w| M \left(\frac{\phi_0^2}{2} - \frac{\phi_0^{n+2}}{n+2} \right) - 2\pi R^2 \rho_L P M \left(\frac{\phi_0^2}{2} - \frac{\phi_0^4}{4} - \frac{\phi_0^{n+2}}{n+2} + \frac{\phi_0^{n+4}}{n+4} \right) + 2\pi R^2 \rho_L N M \left(\frac{\phi_0^2}{2} - \frac{\phi_0^{n+2}}{n+2} - \frac{\phi_0^{n+4}}{n+4} + \frac{\phi_0^{2n+4}}{2n+4} \right) = 0 \tag{11}$$

where,

$$N = \frac{R^2}{v_t} \times \frac{\bar{\varepsilon}_G g}{n(n+2)} \tag{12}$$

and

$$P = \frac{R^2}{v_t} \left(\frac{\tau_w}{2R\rho_L} + \frac{\bar{\varepsilon}_G g}{2n} \right) \tag{13}$$

and

$$M = \bar{\varepsilon}_G \left(\frac{n+2}{n} \right) \tag{14}$$

m is dependent on $t v$ and therefore $t v$ is firstly guessed in Equation 11 and then recalculated using Equation 9 until both the guessed value and the calculated value are the same. This was done using a Microsoft spreadsheet, assuming that $n = 2$. The axial dispersion coefficient can be defined by Fick's law of diffusion:

$$\dot{N}_B = -E_z A \frac{dC_B}{dZ} \tag{15}$$

where \dot{N}_B & is the molar flux, E_z is the axial dispersion coefficient and C_B is the concentration of substance B. The molar flux can also be obtained from a molar balance in the upwards direction:

$$\dot{N}_B = \frac{m_{upwards}}{\rho_L} (C_{B2} - C_{B1}) \quad (16)$$

In differential form, Equation 16 is equivalent to Equation 17:

$$\dot{N}_B = \frac{m_{upwards}}{\rho_L} \left(-\frac{dC_B}{dZ} \Delta Z \right) \quad (17)$$

As the height of a circulation cell is equal 1.4 times the column diameter, Equation 17 is simplified to:

$$\dot{N}_B = -\frac{m_{upwards}}{\rho_L} 1.4D_c \frac{dC_B}{dZ} \quad (18)$$

Comparing Equation 15 with Equation 18, the axial dispersion coefficient is given by:

$$E_z = \frac{1.4D_c m_{upwards}}{\rho_L A} \quad (19)$$

Similarly, the radial dispersion coefficient can be estimated from Equation 20:

$$E_r = \frac{m_{upwards}}{2\pi r_o D_c \rho_L} \times \delta \quad (20)$$

MODEL VERIFICATION

Figure 4 shows a comparison between the estimated kinematic turbulent viscosity and published experimental kinematic turbulent viscosity data. The experimental kinematic turbulent viscosities were measured in column diameters varying between 0.1 to 0.25 m. The predicted kinematic turbulent viscosity is comparable to most of the experimental values from the literature. The percentage error when comparing the estimated kinematic turbulent viscosity with the literature values is as follows: the error was in the range of 35.4–52.6% when comparing the estimated values with those of Miyauchi & Shyu (1970); 0.9–29% for those of Hills (1974); 18.4% for those of Yashitome (1967); 2.2–33% for those of Pavlov (1974) and 35.2% for those of Yamagoshi (1969).

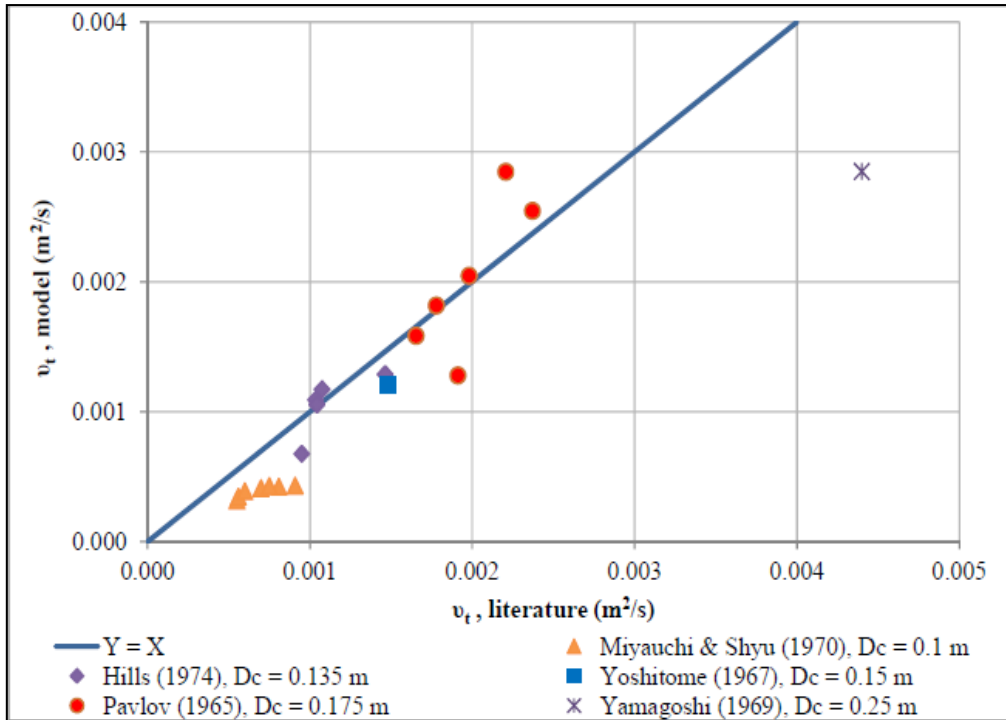


Figure 4: Comparison of predicted and experimental kinematic turbulent viscosity

Figure 5 shows the axial dispersion coefficients values predicted by the model. It was found that at a fixed average gas holdup the axial dispersion coefficient is directly proportional to the column diameter to the power 1.5.

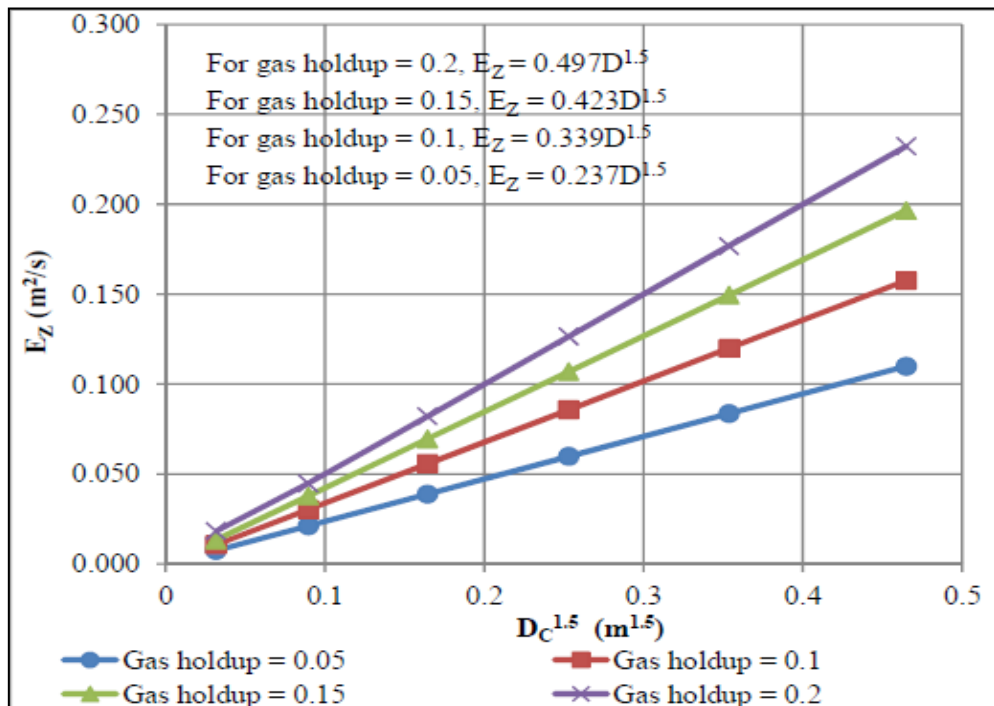


Figure 5: Predicted axial dispersion coefficient as a function of column diameter and gas holdup

Figure 6 shows the calculated axial dispersion coefficients as function of the specific energy dissipation rate and column diameter plotted on a log-log scale using the same form of correlation as Baird & Rice (1975).

As stated before, the height of the circulation cell was assumed to be 1.4 times the column diameter and the value of the exponent used for the gas holdup profile was assumed to be equal to 2. The gas holdup used in the calculations was estimated from the correlation given by Equation 21 reported by Akita & Yoshida (1973).

$$\frac{\bar{\epsilon}_G}{(1 - \bar{\epsilon}_G)^4} = 0.2(gD_c^2 \rho_L / \gamma)^{1/8} (gD_c^3 / \mu_L^2)^{1/12} (u_G / \sqrt{gD_c^2}) \tag{21}$$

This correlation for gas holdup was developed from data for various gas–liquid systems and it also agrees reasonably well with the gas holdup data reported by Ueyama & Miyauchi (1977). Axial dispersion coefficients were calculated for column diameters from 0.1 to 0.6 m and superficial gas velocities from 0.03 to 12 m/s. The calculated results were then correlated against the abscissa using a simple power law (i.e. the dashed line).

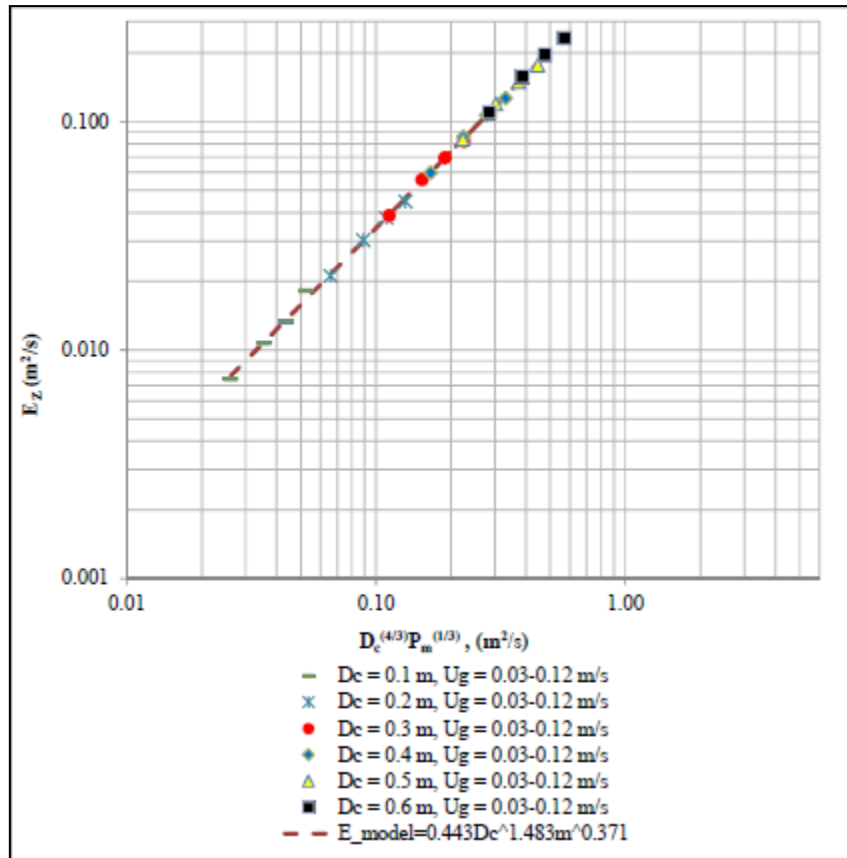


Figure 6: Predicted axial dispersion coefficient

Figure 7 shows the power law correlation for the axial dispersion coefficient with experimental data plotted on a log-log graph as reported by Baird & Rice (1975). The power law correlation and Fig. 7 were prepared in order to compare the estimated axial dispersion coefficients derived from the mechanistic model with the reported experimental data which unfortunately did not include any information on gas holdup which is a required parameter used in the mechanistic model. The power law correlation is similar to the correlation of Baird & Rice (the solid line) but has a slightly higher slope. It can be seen that it fits the experimental data reasonably well and seems to predict the trend over the range of reported values slightly better than the correlation of Baird & Rice.

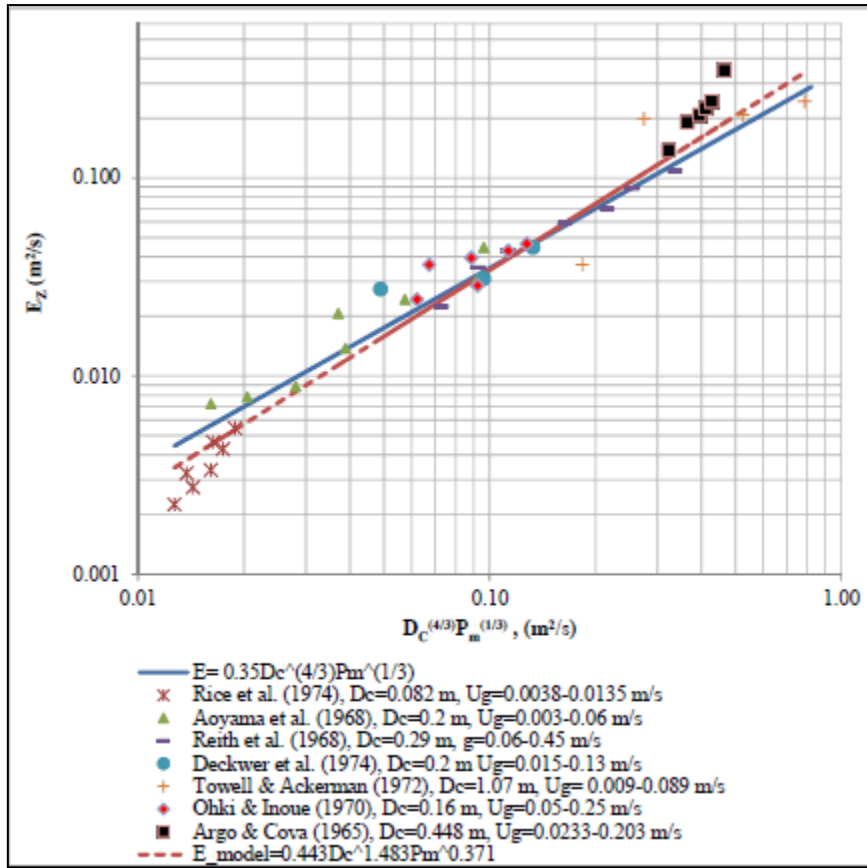


Figure 7: Experimental axial dispersion coefficients from the literature (Baird & Rice, 1975)

Table 1 compares the ratios of the axial to radial dispersion coefficients obtained with the model with those reported in the literature. The ratios obtained are in the range of 23.6 to 24.7 and are of the same order of magnitude than the values reported in the literature.

Table 1: Ratios of axial to radial dispersion coefficient

Model $0.03 \leq u_G \leq 0.12 m$	Deckwer (1992)	Abdulrazzaq (2010)	Camacho Rubio et al (2004)
23.6–24.7	10	50–100	100

CONCLUSIONS

A mechanistic model that is based on the underlying physical phenomena occurring in a bubble column was developed for estimating kinematic turbulent viscosity, axial and radial dispersion coefficients. Although the model is a gross over simplification of reality, its extrapolation to regions outside the range of experimental verification seems intuitively more realistic than extrapolation of purely empirical models. Furthermore, the model provides insight into how mass and momentum exchange occurs in a bubble column.

The model was developed by assuming that the main cause of momentum and mass exchange in bubble columns is the presence of large circulation cells. The turbulent viscosity was estimated from the product of the mass flux across and penetration depth. The height of the circulation cells was found to be approximately equal

to 1.4 times the column diameter and penetration depth was approximately equal to half of the column radius. The predicted kinematic turbulent viscosities agreed reasonably well with the experimental values reported in the literature and the estimated axial dispersion coefficients are also within the range of those reported in the literature. Lastly, the model predicts that the ratio of axial to radial dispersion coefficient is of the same order of magnitude as the small number of values reported in the literature.

NOMENCLATURE

C_B	concentration for substance B	[mol/m ³]
D_C	column diameter	[m]
E_r	radial dispersion coefficient	[m ² /s]
E_z	axial dispersion coefficient	[m ² /s]
g	gravitational acceleration	[m/s ²]
G	mass flux across the curved surface where the liquid velocity is zero	[kg.s ⁻¹ .m ⁻²]
m_{upwards}	liquid mass flowrate in the upwards direction of the circulation cell	[m]
N_B	molar flux	[mol/m]
n	constant in gas holdup equation	[–]
P	pressure	[Pa]
P_m	energy dissipation rate per unit mass	[m ² /s ³]
r	radial coordinate	[m]
r_0	column radius where liquid velocity is zero	[m]
R	column radius	[m]
u	interstitial liquid velocity	[m/s]
u_w	liquid interstitial velocity at the wall	[m/s]
ΔZ	height of recirculation cell	[m]

Greek letters

ε_G	gas holdup as a function of a column radius
$\bar{\varepsilon}_G$	average gas holdup
ρ_L	liquid density
τ	shear stress
τ_w	shear stress at the wall
μ_L	viscosity of the liquid phase
μ_t	turbulent viscosity

ν_t	kinematic turbulent viscosity
δ	distance travelled by lump of fluid for it to change momentum
γ	surface tension of the liquid

Subscripts

C	critical or column
G	gas
L	liquid
r	radial coordinate or riser
t	turbulent
W	wall
Z	axial coordinate

REFERENCES

1. Abdulrazzaq, B.S. (2010) Investigation measurement of dispersion coefficient and mixing times in bubble column. *Diyala Journal of Engineering Sciences*, 3(2), 97–112.
2. Akita, K. and Yoshida, F. (1973) Gas Holdup and Volumetric Mass Transfer Coefficient in Bubble Columns. *Industrial Engineering Chemistry Process Design and Development*, 12(1), 76–80.
3. Baird, M.H.I. and Rice, R.G. (1975) Axial dispersion in large unbaffle columns. *The Chemical Engineering Journal*, 9, 171–174.
4. Camacho Rubio, F., Sánchez Mirón, A., Cerón García, M.C., García Camacho, F., Molina Grima, E. and Chisti, Y. (2004) Mixing in bubble columns: a new approach for characterizing dispersion coefficients *Chemical Engineering Science*, 59, 4369–4376.
5. Deckwer, W.D. (1992) *Bubble column reactors*. Wiley, Chichester, 113–156.
6. Degaleesan, S. and Dudukovik, M.P. (1998) Liquid backmixing in bubble columns and the axial dispersion coefficient *American Institute of Chemical Engineers Journal*, 44(11), 2369–2378.
7. Degaleesan, S., Roy, S., Kumar S.B. and Dudukovid, M.P. (1996) Liquid mixing based on convection and turbulent dispersion in bubble columns *Chemical Engineering Science*, 51(10), 1967–1976.
8. Ekambara, K. and Joshi, J.B. (2003) CFD simulation of mixing and dispersion in bubble columns, *Transactions of the Institution of Chemical Engineers*, 81(A), 987–1002.
9. Groen, J.S., Oldeman, R.G.C., Mudde, R.F. and Van den Akker, H.E.A. (1996) Coherent structures and axial dispersion in bubble column reactors. *Chemical Engineering Science*, 51(10), 2511–2520.
10. Gupta, P., Ong, B., Al-Dahhan, M.H., Dudukovic, M.P. and Toseland, B.A. (2001) Hydrodynamics of churn turbulent bubble columns: Gas-liquid recirculation and mechanistic modelling. *Catalysis Today*, 64, 253–269.
11. Hills, J.H. (1974) Radial non-uniformity of velocity and voidage in a bubble column. *Transactions of the Institution of Chemical Engineers*, 52, 1.
12. Joshi, J.B. and Sharma, M.M. (1979) A circulation cell model for bubble columns. *Transactions of the Institution of Chemical Engineers*, 57, 244–251.
13. *Transactions of the Institution of Chemical Engineers*, 57, 244–251.

14. Joshi, J.B., Vitankar, V.S., Kulkarni, A.A., Dhotre, M.T. and Ekambara, K. (2002) Coherent flow structures in bubble column reactors (Review papers). *Chemical Engineering Science*, 57, 3157–3183.
15. Krishna, R., Wilkinson, P.M. and Van Dierendonck, L.L. (1991) A model for gas holdup in bubble columns incorporating the influence of gas density on flow regime transitions. *Chemical Engineering Science*, 46(10), 2491–2496.
16. Lakota, A., Jazbec, M. and Levec, J. (2001) Impact of structured packing on bubble column mass transfer characteristics. Part 1. Back mixing in the liquid phase. *Acta Chimica Slovaca*, 48, 453–468.
17. Mena, P.C., Ruzicka, M.C., Rocha, F.A., Teixeira, J.A. and Drahoš, J. (2005) Effect of solids on homogeneous-heterogeneous flow regime transition in bubble columns. *Chemical Engineering Science*, 60, 6013–6026.
18. Millies, M. and Mewes, D. (2005) Back-mixing of the continuous phase in bubble columns *Chemical Engineering Science*, 50(13), 2107–2115.
19. Miyauchi, T. and Shyu, C.N. (1970) Flow of fluid in a gas bubble column. *Kagaku Kogaku*, 34, 958.
20. Pavlov, V.P. (1965) *Tsirkulyatsiya Zhidkosti v Barbotazhnom Apparate Periodichesko deistviya Khim. Prom*, 9, 698.
21. Ruthiya, K.C. (2005) Mass transfer and hydrodynamics in catalytic slurry reactors. Thesis (PhD), Eindhoven Netherlands: Eindhoven University of Technology.
22. Ruzicka, M.C., Zahradnik, J., Drahos, J. and Thomas, N.H. (2001) Homogeneous– heterogeneous regime transition in bubble columns. *Chemical Engineering Science*, 56, 4609–4626.
23. Shaikh, A. and Al–Dahhan, M. (2005) Characterization of the hydrodynamic flow regime in bubble columns via computed tomography. *Flow Measurement and Instrumentation*, 16, 91– 98.
24. Singh, M.K. and Majumder, K.S. (2010) Theoretical study on effect of operating parameters on mass transfer in bubbly flow. *Journal of Engineering and Applied Science*, 5(2), 163–170.
25. Ueyama, K. and Miyauchi, T. (1979) Properties of recirculation turbulent two phase flow in gas bubble columns. *AIChE Journal*, 25(2), 258–266.
26. Ueyama, K. and Miyauchi, T. (1977) Behaviour of bubbles and Liquid in Bubble Column. *Kagaku kogaku ronbunshu*, 3(1), 19–23.
27. Vinit, P.C. (2007) Hydrodynamics and mass transfer in slurry bubble columns: Scale and pressure effects. Thesis (PhD). Eindhoven, Netherlands: Eindhoven University of Technology.
28. Yamagoshi, T. (1969) Thesis (BSc). Japan: University of Tokyo, Department of Chemical Engineering.
29. Yashitome, H. (1967) Dissertation (Dr. Eng). Japan: Tokyo Institute of Technology.